Eidgenössische Technische Hochschule Zürich
Swiss Federal Institute of Technology Zurich

Seminar for Applied Mathematics SAM

Dual Mesh Operator Preconditioning On 3D Screens: Low-Order Boundary Element Discretization.

R. Hiptmair and C. Urzúa-Torres

Research Report No. 2016-14
February 2016

Seminar für Angewandte Mathematik
Eidgenössische Technische Hochschule
CH-8092 Zürich
Switzerland

Funding: ETH grant ETH-04 13-2

Dual Mesh Operator Preconditioning On 3D Screens: Low-Order Boundary Element Discretization.

Ralf Hiptmair* Carolina Urzúa-Torres†

Abstract

We provide key estimates that provide the theoretical foundation for dual mesh operator preconditioning [3] of the weakly singular boundary integral operator and the hypersingular boundary integral operator arising from $-\Delta$ on screens in $\mathbb{R}^3$. For each related boundary integral equation (BIE), this entails the construction of a dual discrete boundary element space (BE space), such that it has the same dimension as its corresponding primal discrete BE space. We discuss this for triangular elements following Buffa and Christiansen [2], and extend their approach also to quadrilateral elements. Furthermore, we adapt Steinbach's work [9] in order to establish mesh assumptions under which our operator preconditioning policy remains applicable to locally refined meshes.

1 Introduction

We consider the following Dirichlet and Neumann boundary value problems (BVPs) in the exterior of a open surface $\Gamma \subset \mathbb{R}^3$,

$$-\Delta U = 0 \quad \text{in } \mathbb{R}^3 \setminus \bar{\Gamma}, \quad U = g \text{ or } \frac{\partial U}{\partial \mathbf{n}} = f \quad \text{on } \Gamma\,, \quad \text{and } |U(\mathbf{x})| = \mathcal{O}(\|\mathbf{x}\|^{-1}) \text{ for } \|\mathbf{x}\| \to \infty, \tag{1}$$

with suitable boundary data g or f.

We use the Boundary Element Method (BEM) to numerically solve these BVPs. By doing so, we convert (1) into *first-kind boundary integral equations* (BIEs) for the unknown jump of the complementary boundary data on Γ. In other words, depending on the case, we will be interested in solving

$$(\mathsf{W}\,\psi)(\mathbf{y}) := \frac{1}{4\pi}\int_\Gamma \psi(\mathbf{x})\frac{\partial^2}{\partial n_{\mathbf{x}}\partial n_{\mathbf{y}}}\frac{1}{\|\mathbf{x}-\mathbf{y}\|}d\Gamma(\mathbf{x}) = f(\mathbf{y}), \qquad \mathbf{y}\in\Gamma,\ \psi \in \widetilde{H}^{1/2}(\Gamma), \tag{2}$$

$$(\mathsf{V}\,u)(\mathbf{y}) := \frac{1}{4\pi}\int_\Gamma \frac{u(\mathbf{x})}{\|\mathbf{x}-\mathbf{y}\|}d\Gamma(\mathbf{x}) = g(\mathbf{y}), \qquad \mathbf{y}\in\Gamma,\ u \in \widetilde{H}^{-1/2}(\Gamma), \tag{3}$$

where $\widetilde{H}^{1/2}(\Gamma)$ be the space of functions whose extension by zero over a closed surface Γ_c containing Γ belongs to $H^{1/2}(\Gamma_c)$ (cf.[7, Chap. 2.4.2]. These Sobolev spaces satisfy the following duality relations

$$\widetilde{H}^{-1/2}(\Gamma) \;\equiv\; (H^{1/2}(\Gamma))' \qquad \text{and} \qquad H^{-1/2}(\Gamma) \;\equiv\; (\widetilde{H}^{1/2}(\Gamma))'. \tag{4}$$

When low-order Galerkin BEM discretization is applied to the above first-kind BIEs, one faces linear systems of equations which are ill-conditioned on fine meshes. Consequently, preconditioning becomes relevant when using iterative solvers to compute the solution of the problems at hand. There are several possible alternatives to design a preconditioner, however, in this report, we will only address dual mesh operator preconditioning.

*Seminar for Applied Mathematics, ETH Zurich, Raemistrasse 101, 8092 Zurich, Switzerland. ralf.hiptmair@sam.math.ethz.ch.

†Seminar for Applied Mathematics, ETH Zurich, Raemistrasse 101, 8092 Zurich, Switzerland. carolina.urzua@sam.math.ethz.ch. This author's work was supported by ETH grant ETH-04 13-2.

Keywords: open surface problems, Laplace equation, operator (Calderón) preconditioning, screen problems

Mathematics Subject Classifications (2010): **65N38**, 65F35, 65F08

In order to use this method for screen problems, one must take into account the additional challenges that appear when the scatterer is an open surface. On the one hand, there are no Calderón identities to build preconditioners. On the other hand, the solutions of our BIEs over Γ present a singular behaviour towards the boundary $\partial\Gamma$ of the open surface. This difficulty can be overcome by using adaptive refinement, however, without preconditioning, this will increase the computational cost of the iterative solvers as the spectral condition numbers of our systems grow like $O(h_{min}^{-1})$, where h_{min} is the size of the smallest cell of the mesh.

In this report we aim to discuss and construct the neccessary discretization tools to apply dual mesh operator preconditioning on simple screens. This means we will follow the precondition strategy proposed in [3, Theorem 2.1], which will be included in the following section for the sake of clarity. Furthermore, we do so by building a dual mesh using Buffa and Christiansen approach [2]. Throughout this report we also consider quadrilateral meshes and some additional discussion regarding their construction is included, although no rigorous analysis is developed.

As mentioned above, we are particularly interested to apply these techniques to tackle non-uniform meshes. Analogously to the 2D case, described in [5, 4], we follow Steinbach's work to prove the inf-sup condition of the L^2 dual pairing for non-uniform meshes. We present 4 possible primal-dual space combinations, although just two of them are of physical interest at the moment.

2 Operator Preconditioning

The construction of our preconditioning strategy is based on the following theorem [3].

Theorem 2.1 (Thm. 2.1 [3])**.** *Let X, Y be reflexive Banach spaces, and let*

$$\mathsf{a} \in \mathcal{L}(X \times X, \mathbb{C}), \qquad \mathsf{b} \in \mathcal{L}(Y \times Y, \mathbb{C}), \qquad \text{and} \qquad \mathsf{t} \in \mathcal{L}(X \times Y, \mathbb{C}),$$

be continuous sesquilinear forms with norms $\|\mathsf{a}\|$, $\|\mathsf{b}\|$, and $\|\mathsf{t}\|$.

If $X_h \subset X$, and $Y_h \subset Y$ are finite-dimensional subspaces such that:

(C1) a, b, *and* t *satisfy discrete inf-sup conditions with constants $c_A, c_B, c_T > 0$, respectively, on the corresponding discrete spaces;*

and,

(C2) *dim X_h = M = dim Y_h;*

choosing any bases $\{\varphi_j\}_{j=1}^{M}$ of X_h, and $\{\phi_i\}_{i=1}^{M}$ of Y_h. Then the associated Galerkin Matrices

$$\mathbf{A}_h := (\mathsf{a}(\varphi_i, \varphi_j))_{i,j=1}^{M}\,, \ \mathbf{B}_h := (\mathsf{b}(\phi_i, \phi_j))_{i,j=1}^{\hat{M}}\,, \ \mathbf{T}_h := (\mathsf{t}(\varphi_i, \phi_j))_{i,j=1}^{M\hat{M}}\,,$$

satisfy

$$\kappa(\mathbf{T}_h^{-1}\mathbf{B}_h\mathbf{T}_h^{-H}\mathbf{A}_h) \leq \frac{\|\mathsf{a}\|\|\mathsf{b}\|\|\mathsf{t}\|^2}{c_A c_B c_T^2}\,, \tag{6}$$

where κ designates the spectral condition number.

In order to establish the building blocks for this theorem, we consider the weak form of the boundary integral operators (BIOs) introduced in (3) and (2) as the sesquilinear forms a, and the standard L^2-scalar product as the dual pairing t.

Moreover, we can choose boundary element spaces (BE spaces) X_h and Y_h to satisfy the condition **(C2)** by defining dual basis functions via Buffa-Christiansen approach [2]. The next section is dedicated to recall some details regarding the construction of this dual discrete space, as well as heuristically extend its concept to quadrilaterals.

The specific characterization of the aforementioned spaces will be defined later, whereas an appropiate sesquilinear form b is out of the scope of this report and will be addressed in a different paper [6]. Still, it is worth mentioning than with all the above ingredients, we will be in a position to formulate our preconditioner as

$$\mathbf{P}_h = \mathbf{T}_h^{-1}\mathbf{B}_h\mathbf{T}_h^{-H}.$$

3 Construction of Discrete Spaces

3.1 Primal, Barycentric and Dual Mesh.

Definition 1. *For a given screen* Γ *in* $\mathbb{R}^3$*, we denote its primal mesh by* Γ_h*.*

We now recall and extend the concept of barycentric refinement from [2] to quadrilaterals by the following definition.

Definition 2. *For each element* $\tau \in \Gamma_h$*:*

(i) Locate its center of mass.

(ii) Compute the centers of the edges of τ*. From now on referred as* mid-edge vertices*.*

(iii) Create the child elements *of* τ *by connecting the original vertices of* τ *and those computed in (i) and (ii) (see Figure 1).*

We define the barycentric refinement $\bar{\Gamma}_h$ *of* Γ_h *as the union of all these children elements.*

Figure 1: Barycentric refinement. On the left, we illustrate the 6 obtained *children elements* for a triangular element, while on the right we show the 4 *children elements* in the case of quadrilaterals. We show the original nodes using red dots, a green diamond for the center of mass and blue x's for the mid-egdes nodes.

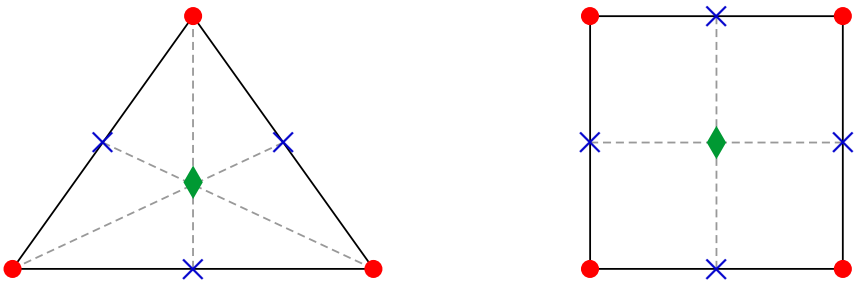

Definition 3. *The union of all barycentric edges connecting mid-edge vertices with centers of mass, create the so called* dual cells*, as shown in Figure 2c.*
We define our dual mesh $\hat{\Gamma}_h$ *to be the union of all the resulting dual cells.*

The fact that these resulting dual elements are unions of barycentric elements, leads us to define the *dual* BE space as a linear combination of *barycentric* basis functions.

Definition 4. *Let* $\bar{X}_h \subset X$ *and* $\bar{Y}_h \subset Y$ *the BE spaces spanned by the basis functions over the barycentric refinement* $\bar{\Gamma}_h$*. Let us introduce the two linking matrices:* [1]

- Coupling matrix $\mathbf{C}_p : \bar{X}_h \to X_h$
  Basis representation of the embedding identity $X_h \to \bar{X}_h$*, since* $X_h \subset \bar{X}_h$*. Therefore, if* $\bar{M}_X := \dim \bar{X}_h$*, and given that* $M = \dim X_h$*, we have that* $\mathbf{C}_p \in \mathbb{R}^{M,\bar{M}_X}$*.*

- Averaging matrix $\mathbf{C}_d : \bar{Y}_h \to Y_h$
  Tells us how to combine the barycentric basis functions of $\bar{Y}_h$ *to get the basis functions of* Y_h *over the dual mesh. Then, in order to establish* $\dim Y_h = M$*, it must hold that* $\mathbf{C}_d \in \mathbb{R}^{M,\bar{M}_Y}$*, where* $\bar{M}_Y := \dim \bar{Y}_h$*.*

[1] We borrow their name from [8]. However, we change the notation for the sake of clarity. $\mathbf{C}_p$ ($\mathbf{C}_d$) stands for primal (dual), to honor the space to which the matrix connects the associated barycentric BE space.

Figure 2: Primal, barycentric and dual meshes. We use black lines to show the primal elements, dashed gray lines for the barycentric elements, and green lines to demarcate the dual cells.

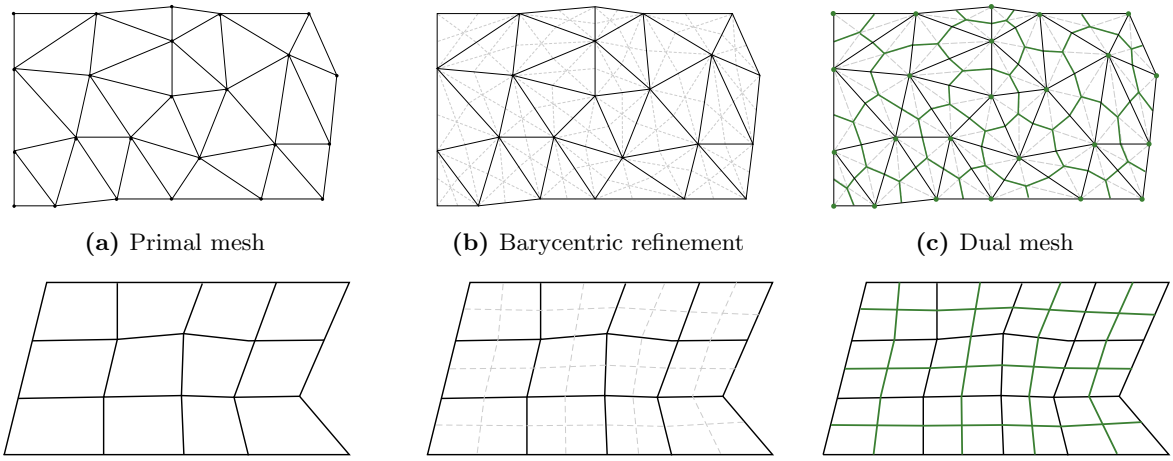

(a) Primal mesh **(b)** Barycentric refinement **(c)** Dual mesh

Here we have slightly abused notation and described these linking matrices as operators. On the one hand, we hope this makes their connection to our preconditioning policy from Theorem 2.1 clearer. On the other hand, we expect it also conveys their functionality regardless of the specific choice of basis functions.

The *averaging matrix* allows us to compute the Galerkin matrix $\mathbf{B}_h$ associated to b over the dual mesh $\hat{\Gamma}_h$: Let $\mathbf{B}_b : \bar{Y}_h \to \bar{Y}_h$ denote the $\bar{M}_Y \times \bar{M}_Y$ Galerkin matrix of b built over the barycentric refinement $\bar{\Gamma}_h$, then $\mathbf{B}_h = \mathbf{C}_d^T \mathbf{B}_b \mathbf{C}_d$, and thus $\mathbf{B}_h \in \mathbb{R}^{M,M}$.

Analogously, the *coupling matrix* helps us to build the Galerkin matrix $\mathbf{T}_h$ associated to the dual coupling t: Let $\mathbf{M}_b : \bar{X}_h \to \bar{Y}_h$ be the $\bar{M}_Y \times \bar{M}_X$ mass matrix computed over the barycentric refinement $\bar{\Gamma}_h$. By using the linking matrices, it is clear that $\mathbf{T}_h = \mathbf{C}_p^T \mathbf{M}_b^T \mathbf{C}_d^T : Y_h \to X_h$, and that it is in $\mathbb{R}^{M,M}$.

3.2 Discretization and notation

Recall that Γ_h denotes the primal mesh, $\hat{\Gamma}_h$ refers to the dual mesh, and $\bar{\Gamma}_h$ is the barycentric refinement.

We build the discrete spaces by choosing low-order Lagrangian boundary element functions. Given a mesh $\Sigma_h \in \{\Gamma_h, \hat{\Gamma}_h, \bar{\Gamma}_h\}$ we use the following notation:

$$\begin{aligned}
\mathcal{S}^{-1,0}(\Sigma_h) &:= \text{ piecewise constants basis functions (characteristic functions),} \\
\mathcal{S}^{0,1}(\Sigma_h) &:= \text{ piecewise linear basis functions (nodal functions),} \\
\mathcal{S}_0^{0,1}(\Sigma_h) &:= \text{ piecewise linear basis functions with zero boundary conditions on } \partial\Gamma \\
&\quad \text{(nodal functions only on internal nodes)}^2.
\end{aligned}$$

We additionally introduce the restricted space $\mathcal{S}_*^{-1,0}(\hat{\Gamma}_h)$ resulting from imposing the condition **(C2)**, i.e. $\dim X_h = \dim Y_h$, when $X_h = \mathcal{S}_0^{0,1}(\Gamma_h)$. We point out that these conditions are enforced via the averaging matrix $\mathbf{C}_d$.

Considering this notation, the 4 combinations of primal and dual spaces are summarized in Table 1. We will dedicate the remainder of this section to discuss the construction of our linking matrices $\mathbf{C}_p$ and $\mathbf{C}_d$ for cases A and B following the techniques from [2], while C and D can be deduced from the other cases.

[2] Also referred as constrained piecewise linear basis functions.

Table 1: Summary of dual pairs of spaces and their discretization. (see Theorem 2.1 for notation).

	Continuous		Discrete	
	X	Y	X_h	Y_h
Case A	$\widetilde{H}^{-1/2}(\Gamma)$	$H^{1/2}(\Gamma)$	$\mathcal{S}^{-1,0}(\Gamma_h)$	$\mathcal{S}^{0,1}(\hat{\Gamma}_h)$
Case B	$\widetilde{H}^{1/2}(\Gamma)$	$H^{-1/2}(\Gamma)$	$\mathcal{S}_0^{0,1}(\Gamma_h)$	$\mathcal{S}_*^{-1,0}(\hat{\Gamma}_h)$
Case C	$H^{-1/2}(\Gamma)$	$\widetilde{H}^{1/2}(\Gamma)$	$\mathcal{S}^{0,1}(\Gamma_h)$	$\mathcal{S}^{-1,0}(\hat{\Gamma}_h)$
Case D	$H^{1/2}(\Gamma)$	$\widetilde{H}^{-1/2}(\Gamma)$	$\mathcal{S}^{-1,0}(\Gamma_h)$	$\mathcal{S}_0^{0,1}(\hat{\Gamma}_h)$

3.3 Linking matrices for triangles

3.3.1 Case A: $X = \widetilde{H}^{-1/2}(\Gamma)$, $Y = H^{1/2}(\Gamma)$

- Coupling matrix $\mathbf{C}_p : \bar{X}_h = \mathcal{S}^{-1,0}(\bar{\Gamma}_h) \to X_h = \mathcal{S}^{-1,0}(\Gamma_h)$

  We aim to connect *primal* piecewise (p.w.) constant basis functions with *barycentric* p.w. constants. Since in both cases the degrees of freedom (dofs) are the element in which the functions are supported, this operator just connects primal elements to barycentric elements.

  Concretely, let N and $\bar{N}$ be the number of elements in Γ_h and $\bar{\Gamma}_h$, respectively. Additionally, consider $\Gamma_h = \bigcup_{i=1}^{N} \tau_i$ and $\bar{\Gamma}_h = \bigcup_{j=1}^{\bar{N}} \bar{\tau}_j$, then

$$\mathbf{C}_p[i,j] = \begin{cases} 1 & \text{if } \bar{\tau}_j \text{ is a child of } \tau_i. \\ 0 & \text{otherwise.} \end{cases} \tag{7}$$

  From where it is clear that each row (primal dof) will have 6 non-zero entries filled with 1 (related barycentric/ children element).

- Averaging matrix $\mathbf{C}_d : \bar{Y}_h = \mathcal{S}^{0,1}(\bar{\Gamma}_h) \to Y_h = \mathcal{S}^{0,1}(\hat{\Gamma}_h)$

Figure 3: Illustration of coefficients of $\mathbf{C}_d$ under Case A using triangular elements. On the left, we present the case when the element is adjacent to the boundary $\partial\Gamma$. On the right, we show the case when the element has a node located on $\partial\Gamma$. N_v (N_w) stands for the number of triangles sharing node v (w). In both situations, $\partial\Gamma$ is indicated by the shaded gray line. We use black lines to indicate primal triangles, green lines for dual cells. Red 'x's designate barycentric nodes.

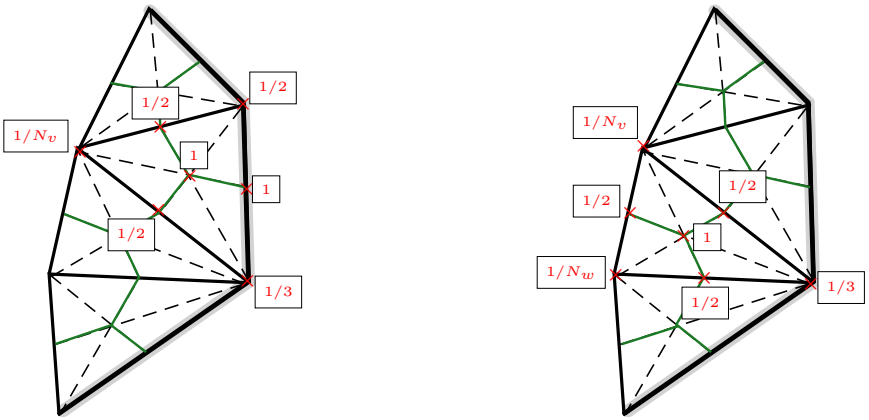

We point out that each dual dof associated to a dual p.w.linear basis function is located in the barycentric vertex corresponding to the center of mass of a primal element. Therefore, each *dual* basis function is a p.w.linear combination of the *barycentric* p.w.linear basis functions defined on the barycentric vertices contained in the primal element to which the center of mass belongs.

Now, the coefficient c_v associated to a barycentric vertex v is given by $c_v = \frac{1}{N_v}$, where N_v equals the number of primal elements that are adjacent to v, which is also the number of dual dofs to which the barycentric node v will contribute. This allows the total contribution of the barycentric dof to the dual BE space to be one.

For the nodes given by the centers of mass, we know that this number will always be one. Analogously, it is always $\frac{1}{2}$ for the internal mid-edge nodes and 1 for those lying in boundary edges. Figure 6 shows a color version of the original illustration of the associated coefficients provided by Buffa and Christiansen [2, Figure 4].

3.3.2 Case B: $X = \widetilde{H}^{1/2}(\Gamma)$, $Y = H^{-1/2}(\Gamma)$.

- Coupling matrix $\mathbf{C}_p : \bar{X}_h = \mathcal{S}_0^{0,1}(\bar{\Gamma}_h) \to X_h = \mathcal{S}_0^{0,1}(\Gamma_h)$

  In this case, the dofs corresponding to constrained primal p.w.linear basis functions are the internal vertices. Furthermore, the *barycentric* dofs associated with each *primal* dof lie in the vertices of the neighbouring barycentric elements.

  As before, the coefficient c_v of each barycentric dof v is such that its total contribution to the primal BE space is one. Therefore, as it is summarized in Figure 4a, we have three possibilities: The barycentric node v is

  – located in the center of the parent triangle: As the barycentric edges connect this node with 3 primal mesh nodes, its coefficient is $c_v = 1/3$.

  – in the middle of an edge: This node is connected with 2 primal mesh nodes. Hence, $c_v = 1/2$.

  – an inherited node: $c_v = 1$, since it will contribute only to itself in the parent mesh.

Figure 4: Illustration of coefficients of $\mathbf{C}_p$ under Case B using triangular elements. We use black lines to indicate primal triangles, green lines for dual cells. Green dots designate primal nodes, and red 'x's barycentric nodes.

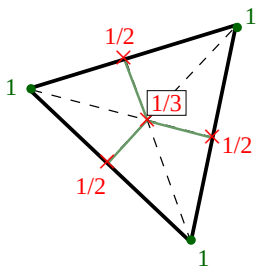

(a) $\mathbf{C}_p$ coefficients associated to the different kind of barycentric nodes.

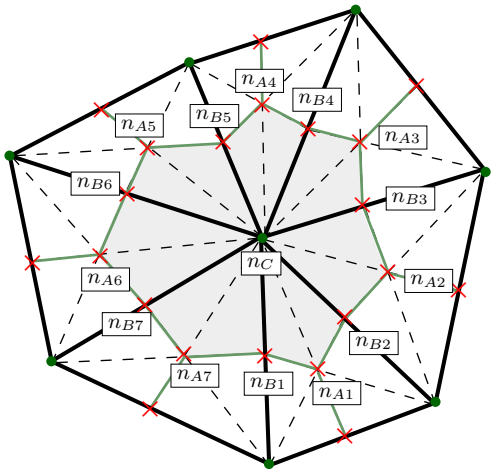

(b) Example of barycentric refinement dofs coupling with a given dual mesh dof (n_C).

Let us illustrate this with the case shown in Figure 4b. There we have

$$\hat{\psi}_{n_C} = \bar{\psi}_{n_C} + \frac{1}{3}\sum_{i=1}^{7} \bar{\psi}_{n_{Ai}} + \frac{1}{2}\sum_{i=1}^{7} \bar{\psi}_{n_{Bi}},$$

where $\hat{\psi}_{n_{(\cdot)}}$ represent p.w.linear basis functions over the dual mesh $\hat{\Gamma}_h$ and $\bar{\psi}_{n_{(\cdot)}}$ p.w.linear basis functions over the barycentric refinement $\bar{\Gamma}_h$.

- AVERAGING MATRIX $\mathbf{C}_d : \bar{Y}_h = \mathcal{S}^{-1,0}(\bar{\Gamma}_h) \to Y_h = \mathcal{S}_*^{-1,0}(\hat{\Gamma}_h)$

  Notice that each dual piecewise constant dof coincides with a vertex of the primal mesh. As we intend to connect *dual* p.w.constant basis functions with *barycentric* p.w.constant basis functions, our matrix has to relate each primal vertex with the barycentric elements that belong to its dual cell. However, as you may observe in Figure 5, such barycentric elements are actually those surrounding the given primal vertex.

  Let $\bar{N}_v$ be the number of barycentric triangles neighbouring the primal vertex v. Then the associated coefficient c_v for said barycentric elements is $c_v = \frac{1}{\bar{N}_v}$.

Figure 5: Illustration of coefficients of $\mathbf{C}_d$ under Case B using triangular elements. We use black lines to indicate primal triangles, green lines for dual cells, green dots for the dofs of the primal and dual meshes (nodes), and a shaded gray line for the boundary $\partial\Gamma$. The green diamonds show the neglected dual mesh dofs at $\partial\Gamma$. Consider node v as the center of the dual mesh filled with gray, $\bar{N}_v$ stands for the number of barycentric triangles neighbouring this node (highlighted by a red 'x').

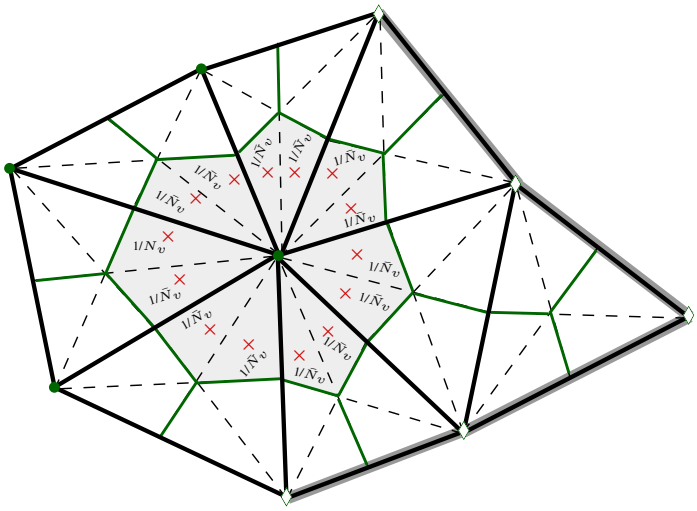

3.4 Definition of linking matrices for quadrilateral elements

Although the following constructions were deduced by analogy to [2], they are just formal and the corresponding analysis has not been carried out yet.

3.4.1 Case A: $X = \widetilde{H}^{-1/2}(\Gamma)$, $Y = H^{1/2}(\Gamma)$.

- Coupling matrix $\mathbf{C}_p : \bar{X}_h = \mathcal{S}^{-1,0}(\bar{\Gamma}_h) \to X_h = \mathcal{S}^{-1,0}(\Gamma_h)$

  Recall from subsection 3.3.2 that we want to link *primal* elements with *barycentric* elements. We do this by applying the same formula (7).

  Therefore, now the resulting matrix has rows with 4 columns equal to 1 (instead of 6), due to the fact that the quadrilateral elements generate 4 barycentric/children elements.

- Averaging matrix $\mathbf{C}_d : \mathcal{S}^{0,1}(\bar{\Gamma}_h) \to \mathcal{S}^{0,1}(\hat{\Gamma}_h)$

  The concept remains the same as before: *dual* dofs correspond to the center of mass of each primal element, while *barycentric* dofs coincide with barycentric vertices.

  Once again, the total contribution of each barycentric basis function must be one, therefore, for a give barycentric vertex v, its coefficient is $c_v = 1/N_v$, where N_v is the number of neighbouring primal elements (to which it will contribute).

Figure 6: Illustration of coefficients of $\mathbf{C}_d$ under Case A using quadrilateral elements. On the left, we present the case when the element is adjacent to the boundary $\partial\Gamma$. On the right, we show the case when the element has a node located on $\partial\Gamma$. N_v (N_w) stands for the number of quadrilateral sharing node v (w). In both situations, $\partial\Gamma$ is indicated by the shaded gray line. We use black lines to indicate primal quadrilaterals, green lines for dual cells. Red 'x's designate barycentric nodes.

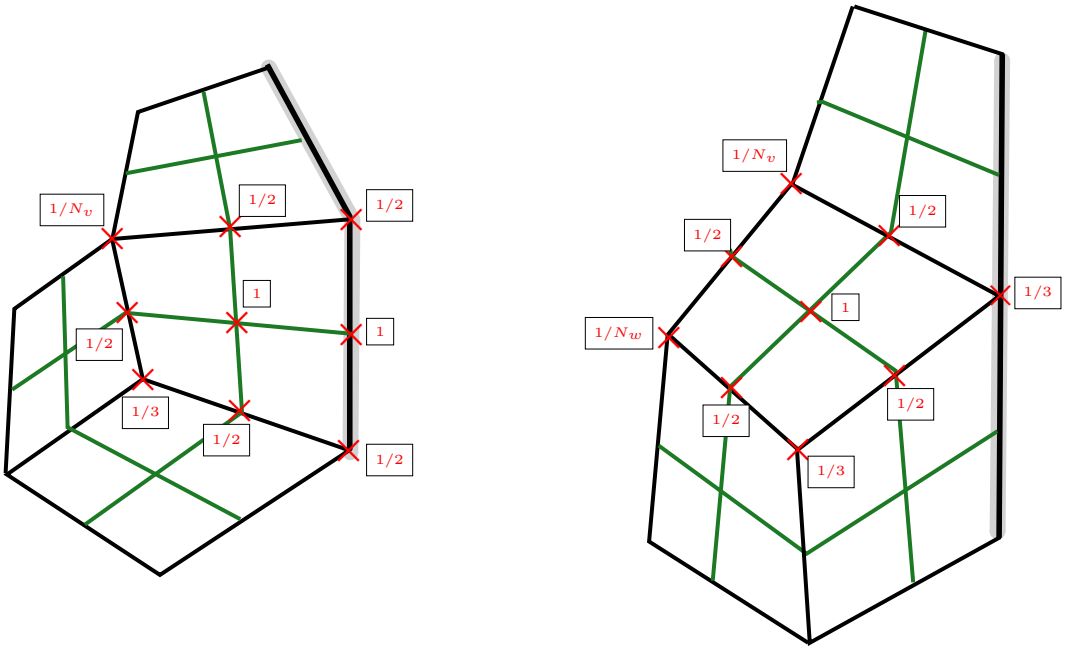

3.4.2 Case B: $X = \widetilde{H}^{1/2}(\Gamma)$, $Y = H^{-1/2}(\Gamma)$.

- Coupling matrix $\mathbf{C}_p : \bar{X}_h = \mathcal{S}_0^{0,1}(\bar{\Gamma}_h) \to X_h = \mathcal{S}_0^{0,1}(\Gamma_h)$

  Recall, we aim to connect the *primal* dofs corresponding to constrained primal p.w.linear basis functions with the *barycentric* dofs associated with each primal dof. This boils down to relate the internal nodes to the nodes of the neighbouring barycentric elements.

Taking into account that the coefficient c_v of each barycentric dof v is such as its contribution to the primal boundary element space is one, we have then three possibilities: Barycentric node v is

- located in the center of the parent quadrilateral: This node is artificially connected with 4 primal mesh nodes, so we get $c_v = 1/4$.
- in the middle of an edge: This node is connected with 2 primal mesh nodes. Hence, its coefficient is $c_v = 1/2$.
- an inherited node: $c_v = 1$, since it will contribute only to itself in the parent mesh.

- AVERAGING MATRIX $\mathbf{C}_d : \bar{Y}_h = \mathcal{S}^{-1,0}(\bar{\Gamma}_h) \to Y_h = \mathcal{S}_*^{-1,0}(\hat{\Gamma}_h)$

  Our matrix is required to connect each primal vertex with the barycentric elements that belong to its dual cell. In other words, using the same a notation as before, each barycentric element neighbouring a primal vertex v will be linked to it with coefficient $c_v = \frac{1}{\bar{N}_v}$.

Figure 7: Illustration of coefficients of linking matrices under Case B using quadrilateral elements. We use black lines to indicate primal triangles, green lines for dual cells, green dots for the dofs of the primal and dual meshes (nodes).

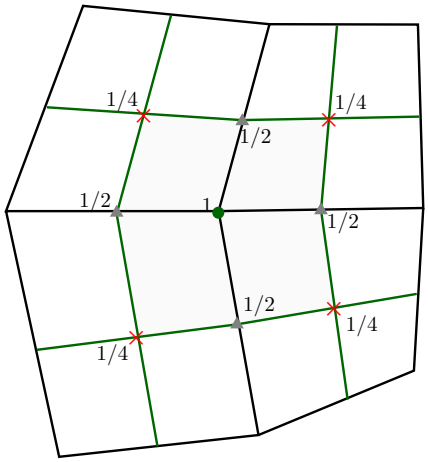

(a) Coupling matrix $\mathbf{C}_p$. We indicate the central node by a red x, the mid-edges nodes by gray triangles and the original nodes by green dots. Next to each node we show the related coefficient.

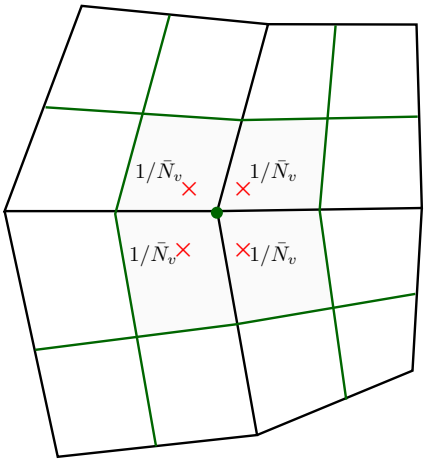

(b) Averaging matrix $\mathbf{C}_d$. Consider node v as the center of the dual mesh filled with gray, $\bar{N}_v$ stands for the number of barycentric triangles neighbouring this node (highlighted by a red 'x').

4 Stability of Discrete Duality Pairing on Non-Uniform Triangular Meshes

The key concept is to establish an inf-sup condition for the dual pairing t, in this case the L^2-inner product over Γ. This entails maintaining the H^1-stability of a generalized L^2-projection $\tilde{Q}_h$, defined via a Petrov-Galerkin approach, as it will be explained later. For this purpose, we adapt the work developed by Steinbach in [9] and introduce some of his notation.

We begin by presenting the mesh assumptions under which we will assert the desired stability results.

Assumption 4.1. *We consider a shape regular and locally quasi-uniform family of primal meshes* $\{\Gamma_h\}_{h\in\mathbb{H}}$, $h > 0$ *of* Γ, *whose members are labelled by* h *from an index set* $\mathbb{H}$.

Let us consider a given primal mesh Γ_h, and denote the mesh-width of an arbitrary element $\tau_l \in \Gamma_h$ by h_l. We equip X_h with the standard locally supported nodal basis functions. As a consequence of

local quasi-uniformity, we can introduce for each basis function $\varphi_k \in X_h$, an associated mesh size $\hat{h}_k$ satisfying

$$\frac{1}{c_Q} \leq \frac{\hat{h}_k}{h_l} \leq c_Q \quad \text{for all } l \text{ such that } \tau_l \cap \operatorname{supp}\{\varphi_k\} \neq \emptyset,\ k = 1, \ldots, M, \tag{8}$$

with a global constant $c_Q \geq 1$.

Let us now define the local trial spaces

$$X_h(\tau_l) := \{\varphi_i^l : \exists \varphi_k \in X_h : \varphi_i^l(x) = \varphi_k(x) \text{ for } x \in \tau_l\} = X_{h|\tau_l},$$
$$Y_h(\tau_l) := \{\phi_i^l : \exists \phi_k \in Y_h : \phi_i^l(x) = \phi_k(x) \text{ for } x \in \tau_l\} = Y_{h|\tau_l}.$$

Let $M_l = \dim X_h(\tau_l) = \dim Y_h(\tau_l)$. We introduce the local Gram matrices as

$$G_l[j,i] = \left\langle \varphi_i^l \,,\, \varphi_j^l \right\rangle_{L^2(\tau_l)}, \quad \text{for } i,j = 1,..,M_l, \tag{9}$$
$$\tilde{G}_l[j,i] = \left\langle \varphi_i^l \,,\, \phi_j^l \right\rangle_{L^2(\tau_l)}, \quad \text{for } i,j = 1,..,M_l, \tag{10}$$
$$\hat{G}_l[j,i] = \left\langle \phi_i^l \,,\, \phi_j^l \right\rangle_{L^2(\tau_l)}, \quad \text{for } i,j = 1,..,M_l. \tag{11}$$

Assumption 4.2 (Assumption 2.1 in [9])**.** *Let $H_l = diag(\hat{h}_k)_{k=1}^{M_l}$, and $D_l := diag(G_l)$. We can find a constant $c_0 > 0$ such that*

$$(H_l \tilde{G}_l^T H_l^{-1} \mathbf{x}_l, \mathbf{x}_l) \geq c_0 \cdot (D_l \mathbf{x}_l, \mathbf{x}_l), \quad \forall \mathbf{x}_l \in \mathbb{R}^{M_l} \tag{12}$$

for all l and h.

Theorem 4.3. *Let Assumptions 4.1 and 4.2 be satisfied. Then, for the following combinations of discrete spaces*

$$\begin{aligned}
&\textit{Case A:} && X_h = \mathcal{S}^{-1,0}(\Gamma_h) \subset X = \widetilde{H}^{-1/2}(\Gamma), && Y_h = \mathcal{S}^{0,1}(\hat{\Gamma}_h) \subset Y = H^{1/2}(\Gamma),\\
&\textit{Case B:} && X_h = \mathcal{S}_0^{0,1}(\Gamma_h) \subset X = \widetilde{H}^{1/2}(\Gamma), && Y_h = \mathcal{S}_*^{-1,0}(\hat{\Gamma}_h) \subset Y = H^{-1/2}(\Gamma),\\
&\textit{Case C:} && X_h = \mathcal{S}^{-1,0}(\Gamma_h) \subset X = H^{-1/2}(\Gamma), && Y_h = \mathcal{S}_0^{0,1}(\hat{\Gamma}_h) \subset Y = \widetilde{H}^{1/2}(\Gamma),\\
&\textit{Case D:} && X_h = \mathcal{S}^{0,1}(\Gamma_h) \subset X = H^{1/2}(\Gamma), && Y_h = \mathcal{S}^{-1,0}(\hat{\Gamma}_h) \subset Y = \widetilde{H}^{-1/2}(\Gamma),
\end{aligned}$$

the discrete inf-sup condition

$$\sup_{v_h \in Y_h} \frac{|\langle w_h \,,\, v_h \rangle|}{\|v_h\|_Y} \geq \frac{1}{c_s} \|w_h\|_X \,, \qquad \forall\, w_h \in X_h. \tag{13}$$

holds with a positive constant c_s independent of h.

Rather than prove Theorem 4.3 as a whole, we split it into the individual cases following the order D-B-C-A. Case D follows as a Corollary of [9, Theorem 2.2], and the same strategy can be applied to prove Case B. Finally, due to duality, cases C and A follow from the first two results and their proof the same as in 2D, already given in [4, 5, Theorem 4.3].

Hence, here we focus on the proof of Case B. This means, given the generalized Galerkin L^2-Projection $\tilde{Q}_h : L^2(\Gamma) \to \mathcal{S}_0^{0,1}(\Gamma_h)$, for a given $u \in L^2(\Gamma)$ defined according to

$$\left\langle \tilde{Q}_h u \,,\, \phi_h \right\rangle_{L^2(\Gamma)} = \langle u \,,\, \phi_h \rangle_{L^2(\Gamma)}, \qquad \forall \phi_h \in \mathcal{S}_*^{-1,0}(\hat{\Gamma}_h), \tag{14}$$

we are interested in its L^2 and H^1 stability. On the one hand, the L^2 stability of $\tilde{Q}_h$ follows from the stability of the L^2 product, given in the following lemma:

Lemma 4.4. *The L^2-stability*

$$\sup_{\psi_h \in \mathcal{S}_*^{-1,0}(\hat{\Gamma}_h)} \frac{|\langle \psi_h \,,\, w_h \rangle|}{\|\psi_h\|_{L^2(\Gamma)}} \geq c_{st} \|w_h\|_{L^2(\Gamma)} \,, \quad \forall\, w_h \in \mathcal{S}_0^{0,1}(\Gamma_h),\ \forall\, h \in \mathbb{H}, \tag{15}$$

where $c_{st} > 0$ independent of h, holds under Assumption 4.1.

Which is a particular case of [9, Lemma 1.7]. On the other hand, the H^1-stability of $\tilde{Q}_h$ is tackled in the following Proposition via a quasi-interpolation operator, as in [9, Section 1.5]. The proof is almost the same as in Steinbach's work except for some small technical details due to the treatment of the tilde spaces and zero boundary conditions. For the sake of completeness, it is provided in the Appendix.

Proposition 4.5. *Let Assumptions 4.1 and 4.2 be satisfied. Then the L^2-projection $\tilde{Q}_h : H_0^1(\Gamma) \to X_h = \mathcal{S}_0^{0,1}(\Gamma_h)$ defined in* (14) *satisfies*

$$\left\| \tilde{Q}_h u \right\|_{H^1(\Gamma)} \leq \tilde{c}_{st} \left\| u \right\|_{H^1(\Gamma)}, \qquad \forall\, u \in H_0^1(\Gamma), \tag{16}$$

with $\tilde{c}_{st}$ a positive constant independent of h.

The remainder of the Theorem's proof for case B follows exactly as in the 2D case [4, 5].

Remark 1. *The stability results discussed in this section are independent of the choice of basis functions. As a consequence, the considered mesh assumptions allow us to lift Buffa and Christiansen's dual discrete space construction on quasi-uniform triangular meshes to non-uniform meshes.*

It might be worth pointing out that in [2, Prop. 3.13], the discrete inf-sup condition (13) *for case B requires global quasi-uniformity together with the following* local non-degeneracy condition *[2, Prop 3.11]:*

Let Γ_h^0 and Γ_h^1 denote the sets of vertices and edges on a given primal mesh Γ_h, respectively. Let N_t denote the number of vertices $v \in \Gamma_h^0$ connected to the vertex $t \in \Gamma_h^0$. The family of meshes $\{\Gamma_h\}_{h\in\mathbb{H}}$ is such that for some $\delta' < 1$ we have for each $h \in \mathbb{H}$ and $s \in \Gamma_h^0$:

$$\sum_{t\in\Gamma_h^0 : \{s,t\}\in\Gamma_h^1} 1/N_t \leq \delta' \tfrac{11}{7}. \tag{17}$$

Proposition 4.6. *For Case B, Assumption 4.1 implies the local non-degeneracy condition* (17).

The proof is given in the Appendix, where the neccessary notation is introduced.

References

[1] J. H. Bramble, J. E. Pasciak, and O. Steinbach, *On the stability of the L^2 projection in $H^1(\Omega)$*, Math. Comp, 71 (2002), pp. 147–156.

[2] A. Buffa and S. Christiansen, *A dual finite element complex on the barycentric refinement*, Mathematics of Computation, 76 (2007), pp. 1743–1769.

[3] R. Hiptmair, *Operator preconditioning*, Computers and Mathematics with Applications, 52 (2006), pp. 699–706.

[4] R. Hiptmair, C. Jerez-Hanckes, and C. Urzúa-Torres, *Optimal operator preconditioning for boundary elements on open curves*, Tech. Rep. 2013-48, Seminar for Applied Mathematics, ETH Zürich, Switzerland, 2013.

[5] R. Hiptmair, C. Jerez-Hanckes, and C. Urzúa-Torres, *Mesh-independent operator preconditioning for boundary elements on open curves.*, SIAM J. Numerical Analysis, 52 (2014), pp. 2295–2314.

[6] R. Hiptmair, C. Jerez-Hanckes, and C. Urzúa-Torres, *Optimal operator preconditioning for hypersingular operator over 3d screens*, Tech. Rep. 2016-09, Seminar for Applied Mathematics, ETH Zürich, Switzerland, 2016. *Submitted to SINUM.*

[7] S. Sauter and C. Schwab, *Boundary Element Methods*, vol. 39 of Springer Series in Computational Mathematics, Springer, Heidelberg, 2010.

[8] Y. Smirnova, *Dual mesh Calderón preconditioning for single layer boundary integral operator*, tech. rep., SAM - Seminar for Applied Mathematics, ETH Zurich, 2012.

[9] O. Steinbach, *Stability estimates for hybrid coupled domain decomposition methods*, vol. 1809 of Lecture Notes in Mathematics, Springer-Verlag, Berlin, 2003.

A Appendix: Stability Proofs

Let N be the number of elements over the primal mesh Γ_h. We define the following basis functions for the primal and dual space defined by Case B:

$$\begin{aligned} X_h &= \mathcal{S}_0^{0,1}(\Gamma_h) = \text{span}\{\varphi_k\}_{k=1}^M, \\ Y_h &= \mathcal{S}^{-1,0}(\hat{\Gamma}_h) = \text{span}\{\phi_k\}_{k=1}^M, \end{aligned}$$

where M is the number of internal nodes on Γ_h, φ_k are "tent functions" such as $\varphi_k(a_j) = \delta_{kj}$ for a given vertex a_j, and ϕ_k are "indicator function" (of an element τ_k).

A.1 Mesh conditions

In Steinbach's original work, the required mesh assumptions where defined as follows

Assumption A.1 (Assumptions 1.1 and 1.2 in [9]). *Let $D_l := \text{diag}(G_l)$. We assume that*

$$c_1^G(D_l\mathbf{x}_l, \mathbf{x}_l) \leq (G_l\mathbf{x}_l, \mathbf{x}_l) \leq c_2^G(D_l\mathbf{x}_l, \mathbf{x}_l), \tag{18}$$

$$c_1^{\tilde{G}}(D_l\mathbf{x}_l, \mathbf{x}_l) \leq (\tilde{G}_l\mathbf{x}_l, \mathbf{x}_l) \leq c_2^{\tilde{G}}(D_l\mathbf{x}_l, \mathbf{x}_l), \tag{19}$$

$$c_1^{\hat{G}}(D_l\mathbf{x}_l, \mathbf{x}_l) \leq (\hat{G}_l\mathbf{x}_l, \mathbf{x}_l) \leq c_2^{\hat{G}}(D_l\mathbf{x}_l, \mathbf{x}_l), \tag{20}$$

hold uniformly for all $\mathbf{x}_l \in \mathbb{R}^{M_l}$, $(l = 1, .., N)$ with positive constants.

Proposition A.2. *Assumption 4.1 implies Assumption A.1*

Proof. This is done by local computations via the reference element (see Figure 8). In order to prove (18) we observe

$$G_l = \frac{\Delta_l}{12}\begin{pmatrix} 2 & 1 & 1 \\ 1 & 2 & 1 \\ 1 & 1 & 2 \end{pmatrix}, \tag{21}$$

with Δ_l is the area of the element τ_l. Then we get the desired condition

$$\frac{1}{2}(D_l\mathbf{x}_l, \mathbf{x}_l) \leq (G_l\mathbf{x}_l, \mathbf{x}_l) \leq 4(D_l\mathbf{x}_l, \mathbf{x}_l). \tag{22}$$

For (19) and (20) we refer to [9, Section 2.2]. □

Figure 8: local primal and dual mesh in reference triangle.

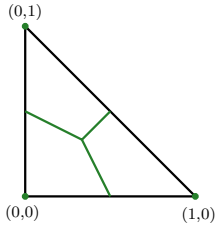

For the sake of clarity, we explicitly work with Assumption A.1 in the subsequent proofs in this appendix.

In addition, for each basis function $\varphi_k \in X_h$ we define the set

$$I(k) := \{l \in \{1, ..., N\} \,:\, \tau_l \cap \text{supp}\,\{\varphi_k\} \neq \emptyset\}, \tag{23}$$

and for each $\tau_l \in \Gamma_h$, the set

$$J(l) := \{k \in \{1, ..., M\} \,:\, \text{supp}\,\{\varphi_k\} \cap \tau_l \neq \emptyset\}. \tag{24}$$

Then we can point out that for Case B, the stability Assumption 4.2 is satisfied if the following local mesh condition:

$$\frac{51}{7} - \sqrt{\sum_{k_1 \in J(l)} \hat{h}_{k_1} \sum_{k_2 \in J(l)} \hat{h}_{k_2}^{-1}} \geq c_0 > 0 \quad \forall \tau_l \in \Gamma_h, \tag{25}$$

holds with a global positive constant c_0 [9, eq. (2.30)]]. The proof is given by Steinbach in [9, Section 2.2].

Proof of Proposition 4.6. We define N_t as the number of vertices s such that $\{s,t\} \in \hat{\Gamma}_h^1$, i.e. the number of vertices connected to t by a dual edge.

Define the dual mesh locally via a reference element (see Figure 8). Then, when computing the local "mixed" Gram mass using Buffa and Christiansen's approach, we get:

$$\tilde{G}_l = \frac{1}{36}\begin{pmatrix} \frac{22}{N_{a^0}} & \frac{7}{N_{a^1}} & \frac{7}{N_{a^2}} \\ \frac{7}{N_{a^0}} & \frac{22}{N_{a^1}} & \frac{22}{N_{a^2}} \\ \frac{7}{N_{a^0}} & \frac{7}{N_{a^1}} & \frac{22}{N_{a^2}} \end{pmatrix} \quad , \quad D_l = \begin{pmatrix} 2 & 0 & 0 \\ 0 & 2 & 0 \\ 0 & 0 & 2 \end{pmatrix}. \tag{26}$$

Here notice that as the basis functions in [2] are normalized, we drop the coefficient $\frac{\Delta_l}{3}$.

Then for any $\mathbf{x}_l = (x_0, x_1, x_2) \in \mathbb{R}^3$

$$2C_1^{\tilde{G}} \sum_{i=0}^{2} x_i^2 \leq \sum_{i=0}^{2} \left(\sum_{j \neq i} x_j x_i \frac{7}{N_{a_i}} + x_i^2 \frac{22}{N_{a_i}} \right) \leq 2C_2^{\tilde{G}} \sum_{i=0}^{2} x_i^2,$$

which holds particularly when

$$\sum_{j=0..2: j \neq i} 1/N_j \leq \delta' \tfrac{22}{7} \frac{1}{N_{a_i}}, \tag{27}$$

i.e. the local version of condition (17). Finally, if one sums this quantity over the $\frac{N_{a_i}}{2}$ primal triangles containing the vertex a_i, one gets the desired non-degeneracy condition. □

A.2 Proof of Proposition 4.5

The proof follows exactly as in the 2D case [4]. The argument slightly changes in some local computations in the proof of the last lemma in this appendix ([4, Lemma B.2]). For the sake of completeness we recall the ingredients here and provide the technical computations for the latter.

Let $\omega_k = \text{supp}\{\varphi_k\}$, then define the related space locally by $X_h(\omega_k) := \{\varphi_j|_{\omega_k} : \varphi_j \in \mathcal{S}_0^{0,1}(\Gamma_h)\}$. Let Q_h^k denote the Galerkin L^2-Projection onto the local trial space $X_h(\omega_k)$, such that for $u \in L^2(\omega_k)$

$$\left\langle Q_h^k u \,,\, v_h \right\rangle_{L^2(\omega_k)} = \left\langle u \,,\, v_h \right\rangle_{L_2(\omega_k)}, \qquad \forall\, v_h \;\in\; X_h(\omega_k). \tag{28}$$

Due to Assumption A.1, we have the stability estimate as well as the quasi optimal error estimate

$$\left\| Q_h^k u \right\|_{L^2(\omega_k)} \leq \|u\|_{L^2(\omega_k)}, \text{ for all } u \in L^2(\omega_k), \tag{29}$$

$$\left\| (\mathsf{Id} - Q_h^k) u \right\|_{L^2(\omega_k)} \leq c_{st}^{loc} \hat{h}_k \, |u|_{H^1(\omega_k)}, \text{ for all } u \in H^1(\omega_k). \tag{30}$$

In particular, local quasi-uniformity gives us the following stability estimate

$$\left\| Q_h^k u \right\|_{H^1(\omega_k)} \leq \tilde{c}_{st}^{loc} \hat{h}_k \, \|u\|_{H^1(\omega_k)} \text{ for all } u \in H^1(\omega_k). \tag{31}$$

Then, it is possible to define a quasi interpolation operator by

$$(P_h u)(x) = \sum_{k=1}^{M} (Q_h^k u)(x_k) \cdot \varphi_k(x), \tag{32}$$

which is also a projection onto $\mathcal{S}_0^{0,1}(\Gamma_h)$. Moreover, P_h have properties which will be key pieces for our proof. We introduce these results in the following two lemmas.

Lemma A.3. (Extension of Lemma 1.9 [9], [4, Lemma B.1]) *Let $u \in H_0^1(\Gamma)$. Then, there exists a positive constant c_{p1} independent of h such that*

$$\|(\mathsf{Id} - P_h) u\|_{L^2(\Gamma)} \leq c_{p1} \sum_{k \in J(l)} \hat{h}_k \, |u|_{H^1(\omega_k)}, \qquad l = 1, \ldots, N, \tag{33}$$

where $J(l)$ is the set of indices of hat functions φ_k that do not vanish on τ_l defined in (24)*. Moreover,*

$$\|P_h u\|_{H^1(\Gamma)} \leq c_{p1} \|u\|_{H^1(\Gamma)}, \quad \textit{for all } u \in H_0^1(\Gamma), \tag{34}$$

and

$$\sum_{k=1}^{M} \hat{h}_k^{-2} \|(\mathsf{Id} - P_h)u\|^2_{L^2(\omega_k)} \leq c_{p1} \|u\|^2_{H^1(\Gamma)}, \quad \textit{for all} u \in H_0^1(\Gamma). \tag{35}$$

Since the only difference with the original Lemma is due to the boundary, where the arguments involved also hold, proof follows from [9, Lemma 1.9].

Lemma A.4. (Extension of Lemma 2.3 [9], [4, Lemma B.2]) *Let condition* (12) *from Assumption 4.2 be satisfied and $\phi_k \in \mathcal{S}_*^{-1,0}(\hat{\Gamma}_h)$, $k = 1, \ldots, M$. Then*

$$\sum_{l=1}^{N} h_l^{-2} \|v_h\|^2_{L^2(\tau_l)} \leq c_{p2} \sum_{k=1}^{M} \left[\frac{\langle v_h \, , \, \phi_k \rangle_{L^2(\Gamma)}}{\hat{h}_k \|\phi_k\|_{L^2(\Gamma)}} \right]^2, \tag{36}$$

for all $v_h \in \mathcal{S}_0^{0,1}(\Gamma_h)$ with a positive constant c_{p2}.

Proof. Again, this proof can be derived by adapting Steinbach's original proof (similarly to what it was shown in [1]). For the sake of clarity, we highlight the main difference from the steps given in [4, Lemma B.2] using bold letters (see local computations almost at the end).

Recall $I(k)$ from (23) as the set of indices of elements τ_l where φ_k is supported; and $J(l)$ from (24). Seeing that $v_h = \sum_{k=1}^{M} v_k \varphi_k \in \mathcal{S}_0^{0,1}(\Gamma_h)$, we can write

$$\begin{aligned}
\sum_{l=1}^{N} h_l^{-2} \|v_h\|_{L^2(\tau_l)} &\leq c_p \sum_{l=1}^{N} h_l^{-2} \sum_{k \in J(l)} v_k^2 \|\varphi_k\|^2_{L^2(\tau_l)} \\
&\leq c_p \sum_{k=1}^{M} v_k^2 \sum_{l \in I(k)} h_l^{-2} \|\varphi_k\|^2_{L^2(\tau_l)} = c_p \sum_{k=1}^{M} v_k^2 \gamma_k^2,
\end{aligned}$$

where $\gamma_k := \sqrt{\sum_{l \in I(k)} h_l^{-2} \|\varphi_k\|^2_{L^2(\tau_l)}}$. Setting $x_k := v_k \gamma_k$ this gives

$$\sum_{l=1}^{N} h_l^{-2} \|v_h\|^2_{L^2(\tau_l)} \leq c_p \|\mathbf{x}\|_2^2.$$

On the other hand,

$$\begin{aligned}
\sum_{k=1}^{M} \left[\frac{\langle v_h \, , \, \phi_k \rangle_{L^2(\Gamma)}}{\hat{h}_k \|\phi_k\|_{L^2(\Gamma)}} \right]^2 &= \sum_{k=1}^{M} \left[\sum_{j=1}^{M} v_j \frac{\langle \varphi_j \, , \, \phi_k \rangle_{L^2(\Gamma)}}{\hat{h}_k \|\phi_k\|_{L^2(\Gamma)}} \right]^2 \\
&= \sum_{k=1}^{M} \left[\sum_{j=1}^{M} x_j \frac{\langle \varphi_j \, , \, \phi_k \rangle_{L^2(\Gamma)}}{\gamma_j \hat{h}_k \|\phi_k\|_{L^2(\Gamma)}} \right]^2 = \|A\mathbf{x}\|_2^2,
\end{aligned}$$

where A is a matrix given by

$$A := D_q^{-1} \tilde{G}_h D_\gamma^{-1}, \qquad D_q := \operatorname{diag}(\hat{h}_k \|\phi_k\|_{L^2(\Gamma)}), \qquad D_\gamma := \operatorname{diag}(\gamma_k).$$

Let $\bar{G}_h = H^{-1} \tilde{G}_h H$. Define for any $\mathbf{y} \in \mathbb{R}^M$

$$b_h := \sum_{k=1}^{M} h_k y_k \varphi_k \in \mathcal{S}_0^{0,1}(\Gamma_h), \qquad q_h := \sum_{k=1}^{M} h_k^{-1} y_k \phi_k \in \mathcal{S}^{-1,0}(\hat{\Gamma}_h).$$

Then, using

$$(H_l^{-1} \tilde{G}_l H_l \mathbf{x}_l, \mathbf{x}_l) \geq c_0 (D_l \mathbf{x}_l, \mathbf{x}_l) \quad \text{for all } \mathbf{x}_l \in \mathbb{R}^{M_l}, \qquad l = 1 \ldots N-1, \tag{37}$$

which is transposed to (12), we derive the following bound:

$$(\bar{G}_h\mathbf{y},\mathbf{y}) = (H^{-1}\tilde{G}_hH\mathbf{y},\mathbf{y}) = (\tilde{G}_hH\mathbf{y},H^{-1}\mathbf{y}) = \langle b_h\,,\,q_h\rangle_{L^2(\Gamma)} = \sum_{l=1}^{N}\langle b_h\,,\,q_h\rangle_{L^2(\tau_l)}$$
$$= \sum_{l=1}^{N}(H_l^{-1}\tilde{G}_lH_l\mathbf{y}_l,\mathbf{y}_l) \geq c_0\sum_{l=1}^{N}(D_l\mathbf{y}_l,\mathbf{y}_l) = c_0(D\mathbf{y},\mathbf{y}).$$

Now, set $D_h^{1/2} := \mathrm{diag}(\|\varphi_k\|_{L^2(\Gamma)})$. From

$$c_0\left\|D_h^{1/2}\mathbf{y}\right\|_2^2 = c_0(D\mathbf{y},\mathbf{y}) \leq (\bar{G}_h\mathbf{y},\mathbf{y}) = (D_h^{-1/2}\bar{G}_h\mathbf{y},D_h^{1/2}\mathbf{y})$$
$$\leq \left\|D_h^{-1/2}\bar{G}_h\mathbf{y}\right\|_2\left\|D_h^{1/2}\mathbf{y}\right\|_2,$$

we conclude that

$$c_0\left\|D_h^{1/2}\mathbf{y}\right\|_2 \leq \left\|D_h^{-1/2}\bar{G}_h\mathbf{y}\right\|_2.$$

Taking $\mathbf{z} := D_\gamma\mathbf{y}$, this is equivalent to

$$c_0\left\|D_h^{1/2}D_\gamma^{-1}\mathbf{z}\right\|_2 \leq \left\|D_h^{-1/2}D_qD_q^{-1}\bar{G}_hD_\gamma^{-1}\mathbf{z}\right\|_2.$$

From the local quasi-uniformity, the ratio of the diagonal entries satisfies

$$\frac{D_h^{1/2}[k,k]}{D_\gamma[k,k]} = \frac{\|\varphi_k\|_{L^2(\Gamma)}}{\sqrt{\sum_{l\in I(k)}h_l^{-2}\|\varphi_k\|_{L^2(\tau_l)}^2}} \geq c\hat{h}_k,$$

due to

$$\frac{D_h^{1/2}[k,k]}{D_\gamma[k,k]} = \frac{\sqrt{\sum_{l\in I(k)}\|\varphi_k\|_{L^2(\tau_l)}^2}}{\sqrt{\sum_{l\in I(k)}h_l^{-2}\|\varphi_k\|_{L^2(\tau_l)}^2}} \geq \frac{1}{\sqrt{\max\limits_{l\in I(k)}h_l^{-2}}} \geq c\hat{h}_k,$$

and

$$\frac{D_q[k,k]}{D_h^{1/2}[k,k]} = \frac{\hat{h_k}\|\phi_k\|_{L^2(\Gamma)}}{\|\varphi_k\|_{L^2(\Gamma)}} \leq c\hat{h}_k.$$

We derive this last result from the fact that $\|\phi_k\|_{L^2(\Gamma)} = \sum_{l\in I(k)}c_lh_l \leq C_Q\hat{h}_k$ **and** $\hat{h}_k = \|\varphi_k\|_{L^2(\Gamma)}$**.**

Thus, by taking $\mathbf{x} = H\mathbf{z}$

$$c_p\|\mathbf{x}\|_2 = c_p\|H\mathbf{z}\|_2 \leq \left\|HD_q^{-1}\bar{G}_hD_\gamma^{-1}\mathbf{z}\right\|_2 = \left\|HD_q^{-1}H^{-1}\tilde{G}_hHD_\gamma^{-1}H^{-1}\mathbf{x}\right\|_2 = \|A\mathbf{x}\|_2.$$

□